Fractional quantum Hall states of Rydberg polaritons

Mohammad F. Maghrebi,[1,2] Norman Y. Yao,[3] Mohammad Hafezi,[1,4] Thomas Pohl,[5]
Ofer Firstenberg,[6] and Alexey V. Gorshkov[1,2]

[1]*Joint Quantum Institute, NIST/University of Maryland, College Park, Maryland 20742, USA*

[2]*Joint Center for Quantum Information and Computer Sceince, NIST/University of Maryland, College Park, Maryland 20742, USA*

[3]*Department of Physics, University of California, Berkeley, California 94720, USA*

[4]*Department of Electrical Engineering and Institute for Research in Electronics and Applied Physics,*
University of Maryland, College Park, Maryland 20742, USA

[5]*Max Planck Institute for the Physics of Complex Systems, 01187 Dresden, Germany*

[6]*Department of Physics of Complex Systems, Weizmann Institute of Science, Rehovot 76100, Israel*

We propose a scheme for realizing fractional quantum Hall states of light. In our scheme, photons of two polarizations are coupled to different atomic Rydberg states to form two flavors of Rydberg polaritons that behave as an effective spin. An array of optical cavity modes overlapping with the atomic cloud enables the realization of an effective spin-1/2 lattice. We show that the dipolar interaction between such polaritons, inherited from the Rydberg states, can be exploited to create a flat, topological band for a single spin-flip excitation. At half filling, this gives rise to a photonic (or polaritonic) fractional Chern insulator—a lattice-based, fractional quantum Hall state of light.

PACS number(s): 42.50.Nn, 32.80.Ee, 42.50.Pq, 73.43.−f

I. INTRODUCTION

Fractional Chern insulators are exotic topological phases of matter that can be thought of as magnetic-field-free fractional quantum Hall states on a lattice [1]. Recently, there have been several proposals to implement fractional Chern insulators in optical flux lattices [2] and dipolar systems [3,4]. On the other hand, recent experimental realizations of topological band structures in arrays of photonic modes [5,6] point to the intriguing possibility of realizing strongly correlated interacting topological states of light [7,8]. Given that photonic systems are prepared and probed differently [9], typically have no chemical potential [10], and exhibit different decoherence mechanisms [11,12] as compared to their electronic counterparts, interacting topological states of light will open new avenues to the study of exotic physics [7]. Furthermore, such states might enable the construction of numerous robust, i.e., topologically protected, optical devices such as filters [7], switches, and delay lines [13,14]. Finally, once such highly nonclassical states of light are released onto freely propagating noninteracting modes, they might be usable as resources for enhanced precision measurements and imaging [15].

While strong interactions between microwave photons are readily achievable [16–21], the realization of strong high-fidelity interactions between optical photons has remained a challenge [22–24]. Only recently, the required strong interaction between optical photons has been implemented in a robust fashion by transforming photons into superpositions of light and highly excited atomic Rydberg states, thus forming polaritons. These polaritons inherit strong dipolar interactions from Rydberg states [25–33] and—together with artificial gauge fields that arise naturally in dipolar systems via the Einstein–de Haas effect [3,34,35]—constitute an ideal platform for realizing interacting topological states of light [36–40].

In this article, we present an example of a fractional Chern insulator of photons (or polaritons) in such a medium. The particular insulator we construct corresponds to the $\nu = 1/2$ filling fraction of the familiar Laughlin fractional quantum Hall state, in which an additional injected polariton fractionalizes into a pair of quasiparticles obeying semionic statistics. In the absence of quantized light, our proposal also allows one to implement fractional Chern insulators of Rydberg atoms.

To understand the basic idea [see Fig. 1(a)], consider a cloud of atoms whose overlaps with spatially separated optical modes form a square lattice (conveniently, an array of traps is not required). Under the conditions of electromagnetically induced transparency (EIT) [41], an auxiliary control field coherently couples a σ^+-polarized photon to a Rydberg state creating a hybrid atom-photon excitation called a Rydberg polariton (call it the $\Downarrow$ polariton) [28,42–45]. Another control field couples a σ^--polarized photon to a different Rydberg state creating the $\Uparrow$ polariton. We populate each site of the lattice (i.e., each optical mode) with exactly one polariton ($\Uparrow$ or $\Downarrow$), turning each site into an effective spin-1/2 particle. Thanks to dipolar Rydberg-Rydberg interactions, the polaritonic spins experience long-range dipolar exchange. Treating the spin-flip operator $|\Uparrow\rangle\langle\Downarrow|$ as a bosonic creation operator, we obtain hardcore bosons hopping on a square lattice. Applied electromagnetic fields can be used to break time-reversal symmetry and to tune Rydberg-Rydberg dipolar interactions into creating topological flat bands for these bosons. In particular, the resulting complex-valued hopping amplitudes endow the bands with nontrivial topology, characterized by a nonzero Chern number of the bands. By analogy with Landau levels, the flatness of the topological band manifests itself in the smallness of the band's dispersion relative to the band gap and allows hardcore interactions to turn a fractionally filled topological band into a fractional Chern insulator. In the language of spins, the $\nu = 1/2$ Laughlin state that we obtain is a gapped chiral spin liquid [46,47]. A limiting case of this proposal corresponds to polaritons consisting entirely of Rydberg excitations, which gives rise to a fractional Chern
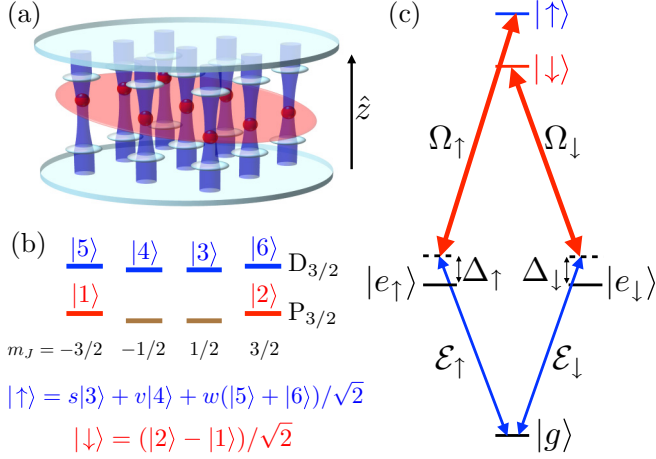
FIG. 1. (Color online) (a) Quasi-two-dimensional cloud of atoms (red disk) overlaps with an array of cavity modes (with cavity axis $\hat{z}$) at a plane tilted relative to $\hat{z}$. The overlaps (red balls) allow one to define a square-lattice array of Rydberg polaritons. Each polariton can be in state $|\Uparrow\rangle$ or $|\Downarrow\rangle$. The resulting spin model has a fractional quantum Hall ground state. (b) To achieve a topological flat-band structure, single-atom dressed states $|\uparrow\rangle$ and $|\downarrow\rangle$ are constructed as linear combinations of several Rydberg levels with spatially dependent coefficients s, v, and w. A weak dc electric field along $\hat{z}$ is assumed. (c) The $|\Uparrow\rangle$ and $|\Downarrow\rangle$ polaritons are created by coupling $|\uparrow\rangle$ and $|\downarrow\rangle$ states to $\mathcal{E}_\uparrow$ (σ^--polarized) and $\mathcal{E}_\downarrow$ (σ^+-polarized) photonic modes, respectively. The flip-flop ($|\uparrow\downarrow\rangle \rightarrow |\downarrow\uparrow\rangle$) dipolar interaction yields the fractional quantum Hall polariton Hamiltonian.

insulator of Rydberg atoms even in the case where each effective spin consists of a single atom.

II. ENGINEERING THE POLARITON HAMILTONIAN

As shown in Fig. 1(a), the atomic cloud is trapped in a plane tilted relative to the cavity axis $\hat{z}$. As we show below, this variable tilt is crucial for obtaining flat topological bands.

As shown in Fig. 1(b), a dc electric field is applied along $\hat{z}$ to remove the degeneracy between Zeeman levels with different $|m_J|$ for Rydberg states $P_{3/2}$ and $D_{3/2}$ (principal quantum numbers will be specified below). At the same time, the field is assumed to be sufficiently weak that the induced dipole moments are negligible. Auxiliary optical and microwave fields can be used to define dressed states $|\downarrow\rangle = (|2\rangle - |1\rangle)/\sqrt{2}$ and $|\uparrow\rangle = s|3\rangle + v|4\rangle + w(|5\rangle + |6\rangle)/\sqrt{2}$, where complex coefficients s, v, and w vary from site to site. The dipolar flip-flop interaction takes two Rydberg atoms in state $|P_{3/2}\rangle |D_{3/2}\rangle$ to state $|D_{3/2}\rangle |P_{3/2}\rangle$. Projecting this interaction onto states $|\uparrow\rangle$ and $|\downarrow\rangle$, we obtain

$$H_I = \sum_{A,B,i \in A, j \in B} t_{ij} \sigma_{\uparrow\downarrow}^i \sigma_{\downarrow\uparrow}^j, \qquad (1)$$

where $\sigma_{\alpha\beta}^i = |\alpha\rangle_i \langle\beta|_i$, A and B label sites of the array, while i and j label atoms. Amplitudes t_{ij} are tuned by adjusting the site dependence of s, v, and w and the direction of $\hat{z}$ relative to the spin lattice.

Following a procedure similar to the one developed in the exciton-polariton literature [48], we will now use Eq. (1) to

derive an interaction between Rydberg polaritons. We start with an ensemble of effective five-level atoms on each site of the square lattice [see Fig. 1(c)]: ground state $|g\rangle$, excited states $|e_\uparrow\rangle$ and $|e_\downarrow\rangle$, and dressed Rydberg states $|\uparrow\rangle$ and $|\downarrow\rangle$ defined above. Since most atoms will remain in state $|g\rangle$, atomic excitations are described using bosonic operators acting on state $|g \ldots g\rangle$ [49,50]. We take $g_{\alpha j} = g_\alpha \sin(\omega_{1,\alpha} z_j/c)$ to be the coupling constant between atom j at position z_j and optical mode A of frequency $\omega_{1,\alpha}$, polarization $\alpha = \uparrow, \downarrow$, and with creation operator $a_{A,\alpha}^\dagger$. We further assume that the two-photon-resonant running-wave control fields of frequency $\omega_{2,\alpha}$ and Rabi frequency Ω_α are propagating along $\hat{z}$. We can then define the following—slowly varying in time—collective operators for site A [49,50]. $\mathcal{E}_{A,\alpha}^\dagger = a_{A,\alpha}^\dagger e^{-i\omega_{1,\alpha}t}$ creates a photon of polarization α, $P_{A,\alpha}^\dagger = (1/g_{A,\alpha}^{col}) \sum_{j \in A} g_{\alpha j} \sigma_{e_\alpha,g}^j e^{-i\omega_{1,\alpha}t}$ creates a collective $|e_\alpha\rangle$ excitation, while $S_{A,\alpha}^\dagger = (1/g_{A,\alpha}^{col}) \sum_{j \in A} g_{\alpha j} \sigma_{\alpha,g}^j e^{-i(\omega_{1,\alpha}+\omega_{2,\alpha})t+i\omega_{2,\alpha}z_j/c}$ creates a collective $|\alpha\rangle$ excitation. Here $g_{A,\alpha}^{col} = \sqrt{\sum_{j \in A} |g_{\alpha j}|^2}$ is the collectively enhanced atom-photon coupling. This collective enhancement is the main reason for using atomic ensembles in place of single atoms as this leads to strong coupling even when individual atoms are coupled to optical modes weakly. In the rotating frame, the noninteracting Hamiltonian (i.e., without H_I) becomes

$$H_0 = \sum_{A,\alpha} -(\Delta_\alpha + i\gamma) P_{A,\alpha}^\dagger P_{A,\alpha} + \left(g_{A,\alpha}^{col} P_{A,\alpha}^\dagger \mathcal{E}_{A,\alpha} \right.$$
$$\left. + \Omega_\alpha S_{A,\alpha}^\dagger P_{A,\alpha} + \text{H.c.}\right), \qquad (2)$$

where Δ_α is the single-photon detuning and 2γ is the decay rate of $|e_\alpha\rangle$. The Hamiltonian can be diagonalized in the dark and bright polariton basis, $H_0 = \sum_{A,\alpha} E_{A,\mathcal{B}_{1\alpha}} \mathcal{B}_{A,1\alpha}^\dagger \mathcal{B}_{A,1\alpha} + E_{A,\mathcal{B}_{2\alpha}} \mathcal{B}_{A,2\alpha}^\dagger \mathcal{B}_{A,2\alpha}$. The dark polariton $\mathcal{D}_{A,\alpha}^\dagger = (g_{A,\alpha}^{col} S_{A,\alpha}^\dagger - \Omega_\alpha \mathcal{E}_{A,\alpha}^\dagger)/\sqrt{|g_{A,\alpha}^{col}|^2 + \Omega_\alpha^2}$ has zero (rotating-frame) energy and thus does not appear in H_0, while the two bright polaritons (linear combinations of $\Omega_\alpha S_{A,\alpha}^\dagger + g_{A,\alpha}^{col} \mathcal{E}_{A,\alpha}^\dagger$ and $P_{A,\alpha}^\dagger$) have large energies (with imaginary parts due to the decay of $|e_\alpha\rangle$). Provided that this energy is larger than the strength of H_I, H_I will be too weak to convert dark polaritons into bright ones, ensuring that the total number of dark polaritons is conserved. Therefore, we can consider the subspace consisting solely of dark polaritons, for which $H_0 = 0$.

Equation (1) mediates dipolar exchange between dark polaritons. The indices i and j belong to different sites since we assume the system starts with one Rydberg excitation per site and since time evolution will not change this. Indeed, intersite hopping of Rydberg excitations requires flip-flops on optical transitions, which are negligible for our intersite separations. The hopping will be further suppressed by the interaction between two Rydberg excitations on the same site. Therefore, using $\sigma_{\uparrow\downarrow}^i = \sigma_{\uparrow g}^i \sigma_{g\downarrow}^i$, the interacting Hamiltonian becomes

$$H = \sum_{A \neq B} t_{AB} \sum_{i \in A} \sigma_{\uparrow g}^i \sigma_{g\downarrow}^i \sum_{j \in B} \sigma_{\downarrow g}^j \sigma_{g\uparrow}^j. \qquad (3)$$

Note that the interaction amplitude t_{AB} depends only on the site index (not on specific atoms) as distances between sites

are much greater than the size of a single site, in analogy with Ref. [51].

We now rewrite the Hamiltonian in terms of collective operators $S_{A,\alpha}^{\dagger}$. For our parameters, for any $j \in A$, $[\sin(\omega_{1,\uparrow} z_j/c)/\sin(\omega_{1,\downarrow} z_j/c)] \exp[i(\omega_{2,\uparrow} - \omega_{2,\downarrow}) z_j/c] \approx 1$ up to an A-dependent phase, which can be absorbed in the definition of $S_{A,\alpha}^{\dagger}$, as shown in the Appendix. One can then check that the Hilbert space spanned on each site by $S_{A,\uparrow}^{\dagger} |g \cdots g\rangle_A$ and $S_{A,\downarrow}^{\dagger} |g \cdots g\rangle_A$ is closed under the action of the Hamiltonian (3), which allows us to rewrite Eq. (3) within this Hilbert space, in the rotating frame, as

$$H = \sum_{A \neq B} t_{AB} S_{A,\uparrow}^{\dagger} S_{A,\downarrow} S_{B,\downarrow}^{\dagger} S_{B,\uparrow}. \qquad (4)$$

We now recall that we are restricted to a subspace consisting of dark polaritons, $|\Uparrow\rangle_A = \mathcal{D}_{A,\uparrow}^{\dagger} |g \cdots g\rangle_A$ and $|\Downarrow\rangle_A = \mathcal{D}_{A,\downarrow}^{\dagger} |g \cdots g\rangle_A$. Since $g_{A,\alpha}^{col} \gg \Omega_\alpha$, the dark polaritons are predominantly composed of Rydberg excitations. The atomic interactions, therefore, directly map onto polariton interactions. Consequently, we arrive at the final polariton Hamiltonian

$$H = \sum_{A \neq B} t_{AB} \mathcal{D}_{A,\uparrow}^{\dagger} \mathcal{D}_{A,\downarrow} \mathcal{D}_{B,\downarrow}^{\dagger} \mathcal{D}_{B,\uparrow}, \qquad (5)$$

which will be used to realize a topological flat band and a fractional Chern insulator by tuning t_{AB}.

III. FRACTIONAL QUANTUM HALL STATES OF RYDBERG POLARITONS

Thinking of $|\Downarrow\rangle$ as vacuum and $|\Uparrow\rangle$ as the presence of a hardcore boson, Eq. (5) describes hopping of such hardcore bosons. The site-dependent parameters s, v, and w are chosen to yield a lattice with a two-site unit cell, as shown in Fig. 2(a). These parameters, together with the direction of $\hat{z}$ relative to the spin lattice, are then tuned (see the Appendix) to achieve a topological flat band for the bosons, as shown in Fig. 2(b). The band's flatness (ratio of band gap to bandwidth) is ≈ 10, while its Chern number is $C = -1$, meaning that the band is topological.
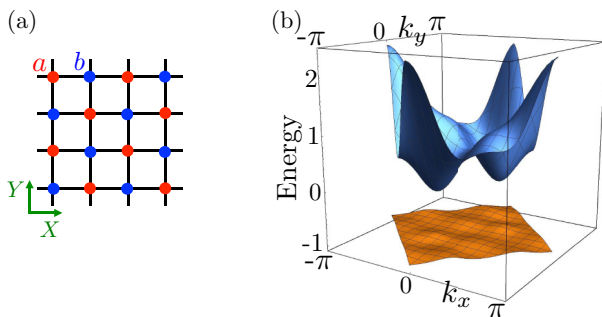

FIG. 2. (Color online) (a) Checkerboard lattice used to create the fractional Chern insulator. The parameters s, v, and w used to define $|\uparrow\rangle$ are different on the two sublattices (a and b). (b) Topological flat band for Rydberg polaritons (Chern number $C = -1$) featuring a flatness ≈ 10.
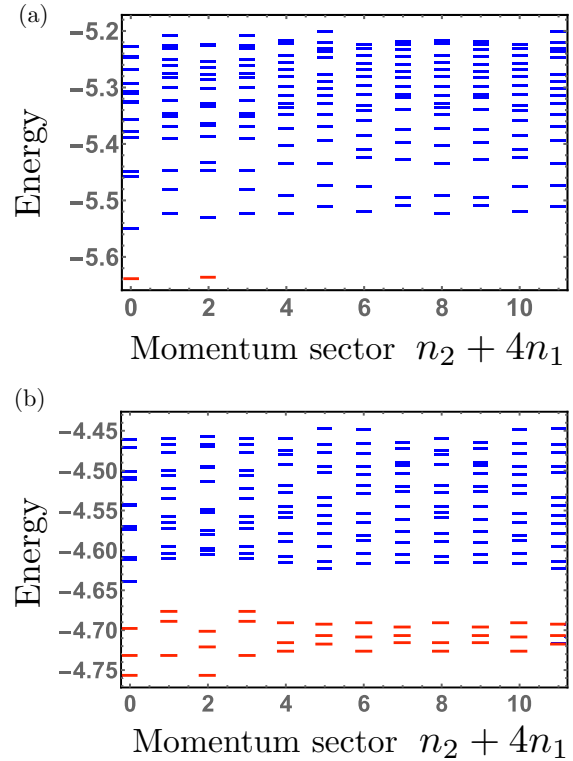

FIG. 3. (Color online) (a) Fractional Chern insulator of Rydberg polaritons. For a 6×4 lattice with six particles with periodic boundary conditions, the eigenstates in momentum sector $n_2 + 4n_1$, where $(k_x, k_y) = (n_1/3, n_2/2 - n_1/3)\pi$, $n_1 = 0,1,2$, and $n_2 = 0,1,2,3$. The two degenerate ground states (red) at $(k_x, k_y) = (0,0)$ and $(0,\pi)$ are separated from the other states by a gap. (b) The momentum-resolved eigenstates for the same parameters as in (a), except now with only five particles instead of six. We observe a clear gap above the 36 low-energy quasihole states (red), in agreement with the quasihole counting formula Q given in the text [1,53].

We now consider filling the band with bosons to a filling $\nu = 1/2$, i.e., half a boson per unit cell. To show that the hardcore interactions alone suffice to produce a fractional Chern insulator, we diagonalized the Hamiltonian (5) on a 6×4 lattice with periodic boundary conditions (we also verified that our results hold for an 8×4 lattice). As shown in Fig. 3(a), we obtain the twofold degenerate ground state separated from the rest of the eigenstates by a gap, consistent with the $\nu = 1/2$ Laughlin state on a torus [52]. As an additional diagnostic, we compute the many-body Chern number. To do this, we numerically calculate the ground-state wave function $|\Psi\rangle$ in the presence of boundary-condition twists (θ_x, θ_y), which are equivalent to inserting fluxes [1]. The many-body Chern number, which is analogous to the Hall conductance, is then defined as $\sigma_{xy} = \frac{1}{2\pi} \int \int F(\theta_x, \theta_y) d\theta_x d\theta_y$, where the many-body Berry curvature is $F(\theta_x, \theta_y) = \text{Im}(\langle \partial_{\theta_y} \Psi | \partial_{\theta_x} \Psi \rangle - \langle \partial_{\theta_x} \Psi | \partial_{\theta_y} \Psi \rangle)$. For both of our degenerate ground states, we find $\sigma_{xy} = -0.5$, consistent with the $\nu = 1/2$ Laughlin state, or equivalently the Kalmeyer-Laughlin chiral spin liquid [46,47].

As yet another diagnostic, in Fig. 3(b), we repeat the diagonalization for the same parameters as in Fig. 3(a) but with one fewer hardcore boson. The low-energy eigenstates, referred to as quasihole states, then provide evidence for the

fractionalization of the removed particle. Indeed, for our fractional quantum Hall state on a torus, the number of such quasihole states is expected to be given by $Q = \binom{N/2+1-N_b}{N/2+1-2N_b} - \binom{N/2-1-N_b}{N/2+1-2N_b}$ [1,53], where N is the number of sites (24 in our case) and N_b is the number of hardcore bosons (five in our case). The numerics presented in Fig. 3(b) show 36 quasihole states in precise agreement with this formula.

IV. EXPERIMENTAL CONSIDERATIONS

In the simplest case of polaritons with vanishing photonic components, we obtain a spin model Eq. (4), where each spin state is a collective Rydberg excitation. The implementation of this purely atomic spin model is a natural intermediate step towards the realization of the polaritonic fractional Chern insulator, a step that can make use of cavity modes for addressing individual collective spins. Such a purely atomic implementation also works with a single atom per site, in which case Eq. (1) immediately yields the desired spin Hamiltonian. Given the strength of Rydberg interactions, this is a promising implementation of fractional Chern insulators in optical lattices [54,55] or microtrap arrays [56,57].

The array of modes can be created using arrays of microlenses [58] or spherical micromirrors [59]. For example [see Fig. 1(a)], two microlens arrays enclosed in a cavity with planar mirrors can support an array of Gaussian modes. Using $69D_{3/2}$ and $70P_{3/2}$ of ^{87}Rb for $|\uparrow\rangle$ and $|\downarrow\rangle$, an $85\,\mu$m lattice constant gives nearest-neighbor dipole-dipole interactions $V_{\text{dd}}/2\pi = 60$ kHz, larger than a reasonable cavity decay rate $\kappa/2\pi \sim 10$ kHz [60] and Rydberg decay rate $\lesssim (2\pi)1$ kHz. The waists of cavity modes, which define the polaritons, are taken to be $<10\,\mu$m, the blockade radius of our Rydberg states. The control fields $\Omega_{\uparrow,\downarrow}$ can be spatially uniform and address all sites globally. The auxiliary optical fields (Rabi frequency Ω_{dr}) used to create the dressed state $|\uparrow\rangle$ are uniform over each site but differ between sites in the checkerboard fashion necessary to create the desired fractional Chern insulator (see the Appendix). We then adopt the following ladder of energy scales: $(\Omega_{\text{dr}}/2\pi = 10\,\text{MHz}) \gg (\Omega_{\uparrow,\downarrow}/2\pi = 2\,\text{MHz}) \gg (\omega_{\text{EIT}}/2\pi = 300\,\text{kHz}) \gg (V_{\text{dd}}/2\pi = 60\,\text{kHz})$. The condition $\Omega_{\text{dr}} \gg \Omega_{\uparrow,\downarrow}$ ensures that the control fields couple to the dark states $|\uparrow\rangle$ and $|\downarrow\rangle$ but not to the bright states. The condition $\Omega_{\uparrow,\downarrow} \gg \omega_{\text{EIT}}$, with $\omega_{\text{EIT}} \sim \Omega_{\uparrow,\downarrow}^2/|\Delta_{\uparrow,\downarrow}|$ the EIT linewidth [41], arises from the requirement $|\Delta_\uparrow - \Delta_\downarrow| \gg \Omega_\downarrow$, which prevents two-photon-resonant coupling of $\mathcal{E}_\uparrow$ to $\Omega_\downarrow$ (see the Appendix). The condition $\omega_{\text{EIT}} \gg V_{\text{dd}}$ ensures that interactions do not violate EIT.

The preparation of the fractional Chern insulator can be achieved as follows. By changing the dc electric-field direction and strength, one first tunes the Hamiltonian to the part of the phase diagram where the ground state is a solid or superfluid, in which each effective spin is in a well-defined state. One then prepares the atomic state corresponding to this solid or superfluid by introducing an appropriate single collective Rydberg excitation onto each lattice site [61]. This can be done by relying on Rydberg blockade and driving a two-photon transition to the Rydberg state [27], where the bottom leg of the transition uses the cavity mode [62]. The site-to-site variations in the collective coupling $g_{A,\alpha}^{\text{col}}$ can be mitigated by using

adiabatic preparation [63,64]. One then changes the parameters of the Hamiltonian (by tuning the dc electric-field strength and direction) to adiabatically go across a phase transition (believed to be continuous [65]) into the fractional Chern insulator phase of collective Rydberg excitations. Finally, the control fields are turned on to adiabatically convert the Rydberg excitations $S_{\downarrow,\uparrow}^\dagger$ into polaritons $|\Downarrow\rangle$, $|\Uparrow\rangle$. The addition of an auxiliary lattice of qubits with fast decay may provide an alternative elegant preparation scheme and may further reduce the effects of photon loss [11].

One detection approach would attempt to flip the polaritons between $|\Downarrow\rangle$ and $|\Uparrow\rangle$ with a variable detuning and variable spatial dependence effectively realizing Bragg spectroscopy and providing the energy- and momentum-dependent spectral function. The spectral function can, in turn, be used to identify gapless chiral Luttinger liquids on the edge [66,67] and a spectral gap in the bulk. Another elegant detection approach, unique to the polaritonic fractional Chern insulators, relies on the retrieval [50,68] of the fractional Chern insulator state onto a purely photonic state of $\mathcal{E}_\uparrow^\dagger$ and $\mathcal{E}_\downarrow^\dagger$ photons. Classical and quantum correlations between the retrieved photons could then be measured using quantum optics techniques and compared to those of the desired fractional Chern insulator [7]. Finally, an elegant combination of preparation and detection would involve first turning on all dressing and control fields to create a "topological filter" [7], and then sending single photons into each cavity; provided the incoming energy matches that of the fractional Chern insulator, the photonic fractional Chern insulator will be transmitted with probability determined by its (small) overlap with the input.

V. OUTLOOK

While we have presented one of the most conceptually straightforward implementations of one of the simplest topological states, the ideas and methods presented in this article point to strongly interacting Rydberg polaritons as a promising and powerful platform for realizing interacting topological states of light. In particular, it should be straightforward to extend to Rydberg polaritons dipolar implementations [69,70] of fractional Chern insulators in flat bands with arbitrary Chern numbers [71,72]. We also expect optical-flux-lattice [2] and Floquet [6] approaches to be extendable to Rydberg polaritons. It is also natural to consider creating interacting topological states of light by trapping ensembles of Rydberg atoms near recently demonstrated arrays of optical-ring resonators supporting topological band structures [5]. Finally, motivated by the exciton-polariton literature [73–75], it would be interesting to consider inducing a nontrivial topology via the atom-photon coupling in the case where, taken separately, atomic and photonic systems are topologically trivial.

We used a separation of energy scales to controllably create a long-range-entangled [76] topological state of polaritons. At the same time, an experimentally more straightforward approach would consist of a free-space setup, in which spatially inhomogeneous control fields give rise to propagating polaritons. Our controllable creation of long-range-entangled topological states will motivate the study of this more complex problem, in which topological and other exotic phenomena may manifest themselves in dynamics.

APPENDIX: DETAILS OF THE EXPERIMENTAL IMPLEMENTATION IN ^{87}Rb

In this Appendix, we first present the details of the experimental implementation in ^{87}Rb, including the construction of dressed states $|\uparrow\rangle$ and $|\downarrow\rangle$ in Fig. 1. We then present the dependence of hopping amplitudes t_{AB} in Eq. (5) on dressing parameters s, v, and w, and give the values of these parameters that were used to construct Figs. 2(b) and 3.

Expanding on Figs. 1(b) and 1(c), on the example of ^{87}Rb, Fig. 4 shows a detailed level structure for constructing dressed states $|\uparrow\rangle = s\,|3\rangle + v\,|4\rangle + w(|5\rangle + |6\rangle)/\sqrt{2}$ and $|\downarrow\rangle = (|2\rangle - |1\rangle)/\sqrt{2}$ and for coupling these states to quantized light fields to form $|\Uparrow\rangle$ and $|\Downarrow\rangle$ Rydberg polaritons. By analogy with Ref. [3], the optical Raman dressing beams coupling state $|4\rangle$ to state $|5\rangle$ and state $|3\rangle$ to state $|6\rangle$ provide the required spatial dependence (to be discussed below) of the
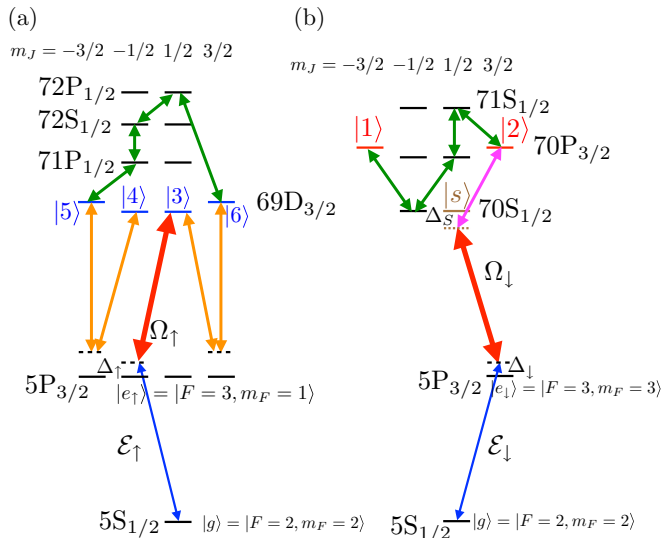

FIG. 4. (Color online) Levels of ^{87}Rb for generating the $\Uparrow$ (a) and $\Downarrow$ (b) polaritons. In particular, $|\uparrow\rangle = s\,|3\rangle + v\,|4\rangle + w(|5\rangle + |6\rangle)/\sqrt{2}$, while $|\downarrow\rangle = (|2\rangle - |1\rangle)/\sqrt{2}$. All the labeled states except for $|e_\uparrow\rangle$ have nuclear spin quantum number $m_I = 3/2$. Green and magenta are microwave fields coupling Rydberg states to Rydberg states. Blue, red, and orange are optical fields coupling $5P$ to $5S$ and to Rydberg states. $|g\rangle = |F=2, m_F=2\rangle = |m_J = 1/2, m_I = 3/2\rangle$; $|e_\downarrow\rangle = |F=3, m_F=3\rangle = |m_J = 3/2, m_I = 3/2\rangle$. The state $|s\rangle$ in (b) is used virtually. The positions of Rydberg levels in (b) relative to those in (a) are drawn to minimize the crowding of the figure: in reality, $69D_{3/2}$ lies between $70P_{3/2}$ and $71S_{1/2}$.

dressing parameters s, v, and w. All the remaining classical fields (control fields $\Omega_\uparrow$ and $\Omega_\downarrow$, as well as microwave fields coupling $|5\rangle$ to $|6\rangle$, $|1\rangle$ to $|2\rangle$, and $|2\rangle$ to $|s\rangle$) are spatially uniform. State $|\uparrow\rangle$ (varying from site to site in a checkerboard fashion as discussed below) in Fig. 4(a) is the dark state of the Raman beams and the four microwave fields, while state $|\downarrow\rangle$ (same on all sites) in Fig. 4(b) is the dark state of the four microwave fields. The $|s\rangle \rightarrow |2\rangle$ microwave field connects the odd-parity P-state $|\downarrow\rangle$ to the even-parity state $70S_{1/2}$, where the latter state is assumed to be detuned ($\Delta_S \gg \Delta_\downarrow$) and is used virtually.

Let us now show explicitly how the Raman dressing beams coupling state $|5\rangle$ to state $|4\rangle$ and state $|3\rangle$ to state $|6\rangle$, together with the microwave dressing fields coupling state $|5\rangle$ to state $|6\rangle$, can turn $|\uparrow\rangle = s\,|3\rangle + v\,|4\rangle + w(|5\rangle + |6\rangle)/\sqrt{2}$ into the dark state (for any desired s, v, and w). In general, consider N "ground" states $|g_1\rangle, \ldots, |g_N\rangle$ coupled to each other with $2N-2$ control fields via $N-1$ intermediate "excited" states $|e_1\rangle, \ldots, |e_N\rangle$ according to the Hamiltonian $H = \sum_{j=1}^N |e_j\rangle\,(\langle g_j|\,\Omega_{j,j} + \langle g_{j+1}|\,\Omega_{j,j+1}) + \text{H.c.}$ [77]. It is clear that this Hamiltonian supports a unique zero-energy dark state $|D\rangle = \sum_j c_j\,|g_j\rangle$ made up of ground states alone, where the amplitudes c_j are set by $c_j/c_{j+1} = -\Omega_{j,j+1}/\Omega_{j,j}$ and can be tuned to arbitrary values by tuning the ratios of the Rabi frequencies. In the case of $|\uparrow\rangle$, the role of the five ground states is played by $|4\rangle$, $|5\rangle$, $|72S_{1/2}, m_J = -1/2\rangle$, $|6\rangle$, and $|3\rangle$, while the role of the excited states is played by the four intermediate states.

We choose a dc electric field of 0.5 V/cm. At this field, the energy difference ΔE_{Stark} between $|1\rangle$ and $|70P_{3/2}, m_J = -1/2\rangle$ is $\approx (2\pi)60$ MHz [while the energy difference between $|4\rangle$ and $|5\rangle$ is much larger: $\sim (2\pi)\,220$ MHz]. At the same time, this dc electric field is sufficiently weak that the admixture of other states into bare states $|1\rangle$, $|4\rangle$, and $|5\rangle$ remains small ($\lesssim 0.2$), justifying the assumption of negligible induced dipole moments and the use (see below) of transition dipole moments corresponding to a vanishing electric field. With $\Delta E_{\text{Stark}}/2\pi = 60$ MHz, we have the following ladder of energy scales: $(\Delta E_{\text{Stark}}/2\pi = 60\,\text{MHz}) \gg (\Omega_{\text{dr}}/2\pi = 10\,\text{MHz}) \gg (\Omega_{\uparrow,\downarrow}/2\pi = 2\,\text{MHz}) \gg (\omega_{\text{EIT}}/2\pi = 300\,\text{kHz}) \gg (V_{\text{dd}}/2\pi = 60\,\text{kHz}) \gg (\kappa/2\pi = 10\,\text{kHz})$. This ladder ensures the following.

(i) The condition $\Delta E_{\text{Stark}} \gg \Omega_{\text{dr}}$ (where Ω_{dr} is the Rabi frequency of the optical and microwave dressing fields) removes the degeneracy between Zeeman levels with different $|m_J|$. This enables the use of frequency selection for addressing desired transitions. For example, this condition ensures that the dressing lasers and microwaves do not Raman couple $|3\rangle$ to $|4\rangle$, or $|70P_{3/2}, m_J = -1/2\rangle$ to $|70P_{3/2}, m_J = 1/2\rangle$. The dc Stark shift also allows us to avoid the two-photon resonant excitation of $|69D_{3/2}, m_J = 3/2, m_I = 1/2\rangle$ (instead of $|3\rangle$) by $\Omega_\uparrow$ since $|m_J = 3/2\rangle$ moves out of two-photon resonance.

(ii) The condition $\Omega_{\text{dr}} \gg \Omega_{\uparrow/\downarrow}$ ensures that the control fields couple to the dark states $|\uparrow\rangle$ and $|\downarrow\rangle$ created by the dressing fields, but not to the bright states.

(iii) The condition $\Omega_{\uparrow/\downarrow} \gg \omega_{\text{EIT}}$ (where $\omega_{\text{EIT}} \sim \Omega_{\uparrow,\downarrow}^2/\Delta_{\uparrow,\downarrow}$ is the EIT linewidth [41]) arises from the requirement $|\Delta_\uparrow - \Delta_\downarrow| \gg \Omega_\downarrow$, which prevents two-photon resonant coupling of $\mathcal{E}_\uparrow$ to $\Omega_\downarrow$. Specifically, we take $\Delta_\uparrow = -\Delta_\downarrow = (2\pi)10$ MHz. Optical elements can then be used to ensure that $\mathcal{E}_\uparrow$ and

$\mathcal{E}_\downarrow$ [whose frequencies $\omega_{1,\uparrow}$ and $\omega_{1,\downarrow}$ thus differ by $(2\pi)20$ MHz] are resonant with cavity modes at their respective polarizations.

(iv) The condition $\omega_{\text{EIT}} \gg V_{\text{dd}}$ ensures that the interactions are not strong enough to violate EIT and to compromise dark-state polaritons.

(v) Finally, the condition $V_{\text{dd}} \gg \kappa$ ensures that the Hamiltonian responsible for the fractional Chern insulator operates on an energy scale larger than the rate at which photons leak out of the cavity. Decay rates at the 10 kHz level are reasonable [60].

It is worth pointing out that, at room temperature, the decay rates of the Rydberg states involved ($69D$, $70S$, and $70P$) are $\gamma_R \lesssim (2\pi)1$ kHz [78], making these rates negligible compared to V_{dd}. It is also worth noting that the implementation of the purely atomic fractional Chern insulator via Eq. (4) requires a much simpler ladder of energy scales since the control Rabi frequency, the EIT linewidth, and cavity decay rate no longer enter: $\Delta E_{\text{Stark}} \gg \Omega_{\text{dr}} \gg V_{\text{dd}} \gg \gamma_R$.

To derive Eq. (4), we assumed that, for any atom j on site A, the condition $[\sin(\omega_{1,\uparrow} z_j/c)/\sin(\omega_{1,\downarrow} z_j/c)]\exp[i(\omega_{2,\uparrow} - \omega_{2,\downarrow})z_j/c] \approx 1$ holds up to an A-dependent phase. We now verify this condition. On a given site, z_j varies at most by the thickness of the atomic cloud, which needs to be smaller than the Rydberg blockade radius, $\approx 10 \ \mu$m, in order to ensure an intrasite excitation blockade. Hence $\exp[i(\omega_{2,\uparrow} - \omega_{2,\downarrow})z_j/c]$ will not vary appreciably with j since $|\omega_{2,\uparrow} - \omega_{2,\downarrow}| \approx (2\pi)17$ GHz, which is the energy separation between $70S$ and $69D$. Now $|\omega_{1,\uparrow} - \omega_{1,\downarrow}| = |\Delta_\uparrow - \Delta_\downarrow| = (2\pi)20$ MHz, while $\omega_{1,\uparrow} = (2\pi)384$ THz (i.e., the D_2 line in ^{87}Rb). Thus, as long as the cavity length is less than ≈ 10 cm, the two modes get <0.01 out of phase with each other, ensuring that $[\sin(\omega_{1,\uparrow} z_j/c)/\sin(\omega_{1,\downarrow} z_j/c)] \approx 1$.

The condition $g_{A,\alpha}^{\text{col}} \gg \Omega_\alpha$, which ensures that the dark polaritons are predominantly composed of Rydberg excitations, is easy to satisfy for our parameters. Indeed, for a mode of length 10 cm and cross section equal to the square of the Rydberg blockade radius [i.e., $\sim(10 \ \mu$m$)^2$], the single-photon Rabi frequency on the $5S_{1/2} \to 5P_{3/2}$ transition of ^{87}Rb is $\sim$MHz. Therefore, collective enhancement (by the square root of the number of atoms coupled to the mode) will easily ensure $g_{A,\alpha}^{\text{col}} \gg \Omega_\alpha$ for $\Omega_\alpha/2\pi = 2$ MHz.

We now derive the dependence of t_{AB} in Eq. (5) on the dressing parameters s, v, and w. Let $\mathbf{d}$ be the dipole-moment operator, so that $d^0 = d^z$ and $d^\pm = \mp(d^x \pm id^y)/\sqrt{2}$ are the three components of the corresponding irreducible spherical tensor. Then, from the Wigner-Eckardt theorem, referring to Fig. 1(b), $-\langle 5|d^0|1\rangle = \langle 6|d^0|2\rangle = \mu_{26} = d\sqrt{3/5}$ and $-\langle 4|d^+|1\rangle = \langle 3|d^-|2\rangle = \mu_{23} = d\sqrt{2/5}$ for some reduced

matrix element d. Taking R to be the distance between Rydberg atoms $i \in A$ and $j \in B$ and dividing by $1/(4\pi\epsilon_0 R^3)$, the dipole-dipole Hamiltonian between spins i and j becomes

$$H_{ij} = (1 - 3\cos^2\theta)\left[d_i^0 d_j^0 + \tfrac{1}{2}(d_i^+ d_j^- + d_i^- d_j^+)\right]$$
$$- \tfrac{3}{2}\sin^2\theta[e^{-2i\phi}d_i^+ d_j^+ + \text{H.c.}], \tag{A1}$$

$$\to (1 - 3\cos^2\theta)\big[\mu_{26}^2(|51\rangle\langle 15| + |62\rangle\langle 26| - |61\rangle\langle 25|$$
$$- |52\rangle\langle 16|) - \tfrac{1}{2}\mu_{23}^2(|32\rangle\langle 23| + |41\rangle\langle 14|)\big]$$
$$- \tfrac{3}{2}\sin^2\theta\big[e^{-2i\phi}\mu_{23}^2(|42\rangle\langle 13| + |24\rangle\langle 31|)\big] + \text{H.c.} \tag{A2}$$

$$\to t_{ij}\sigma_{\downarrow\uparrow}^i \sigma_{\downarrow\uparrow}^j + \text{H.c.}, \tag{A3}$$

where

$$t_{ij} = (1 - 3\cos^2\theta)\big[\mu_{26}^2 w_i^* w_j - \tfrac{1}{4}\mu_{23}^2(s_i^* s_j + v_i^* v_j)\big]$$
$$+ \tfrac{3}{4}\sin^2\theta\,\mu_{23}^2(e^{-2i\phi}v_i^* s_j + e^{2i\phi}v_j s_i^*) \tag{A4}$$

and where the first "$\to$" projects the Hamiltonian onto states $|1\rangle$ through $|6\rangle$, while the second "$\to$" projects the Hamiltonian onto states $|\uparrow\rangle$ and $|\downarrow\rangle$. The first projection is dictated by energy conservation and relies on the fact that the strength of dipole-dipole interaction between two sites is smaller than the splitting between different $|m_J|$ introduced by the dc electric field [77,79,80]. The second projection is also dictated by energy conservation and relies on the fact that the auxiliary dressing fields used to define $|\uparrow\rangle$ and $|\downarrow\rangle$ split these two (dark) states from all the other (bright) states by an energy larger than the strength of dipole-dipole interaction between two sites [77,79,80].

Finally, we present the specific values of s, v, and w that were used to obtain Figs. 2(b) and 3. As in Ref. [3], we consider a checkerboard lattice, shown in Fig. 2(a), consisting of an a sublattice and a b sublattice, so that parameters s, v, and w are different on the two sublattices. Specifically, we parametrize $s_{a/b} = \sin(\alpha_{a/b})\sin(\theta_{a/b})$, $v_{a/b} = \sin(\alpha_{a/b})\cos(\theta_{a/b})e^{i\phi_{a/b}}$, and $w_{a/b} = \cos(\alpha_{a/b})e^{i\gamma_{a/b}}$. For Figs. 2(b) and 3, we chose $\{\theta_a, \theta_b, \phi_a, \phi_b, \alpha_a, \alpha_b, \gamma_a, \gamma_b\} = \{0.87, 1.01, 2.79, 3.44, 2.37, 1.31, 4.71, 6.35\}$. We make a further modification by changing the sign of w_a and w_b every other row [this is not shown in Fig. 2(a)]. Without increasing the size of the unit cell (two sites), this modification plays an important role in allowing us to flatten the topological band. Finally, in Figs. 2(b) and 3, $\Theta_0 = 0.68$ and $\Phi_0 = 2.60$ are, respectively, the polar and the azimuthal angles of the dc electric field ($\hat{z}$) in the coordinate system determined by the X-Y plane in which the square lattice is sitting.

[1] N. Regnault and B. A. Bernevig, Phys. Rev. X **1**, 021014 (2011).

[2] N. R. Cooper and J. Dalibard, Phys. Rev. Lett. **110**, 185301 (2013).

[3] N. Y. Yao, A. V. Gorshkov, C. R. Laumann, A. M. Läuchli, J. Ye, and M. D. Lukin, Phys. Rev. Lett. **110**, 185302 (2013).

[4] J. Yuen-Zhou, S. K. Saikin, N. Y. Yao, and A. Aspuru-Guzik, Nature Mater. **13**, 1026 (2014).

[5] M. Hafezi, S. Mittal, J. Fan, A. Migdall, and J. M. Taylor, Nat. Photon. **7**, 1001 (2013).

[6] M. C. Rechtsman, J. M. Zeuner, Y. Plotnik, Y. Lumer, D. Podolsky, F. Dreisow, S. Nolte, M. Segev, and A. Szameit, Nature (London) **496**, 196 (2013).

[7] M. Hafezi, M. D. Lukin, and J. M. Taylor, New J. Phys. **15**, 063001 (2013).

[8] R. O. Umucalilar and I. Carusotto, Phys. Lett. A **377**, 2074 (2013).

[9] A. Aspuru-Guzik and P. Walther, Nat. Phys. **8**, 285 (2012).

[10] M. Hafezi, P. Adhikari, and J. M. Taylor, arXiv:1405.5821.

[11] E. Kapit, M. Hafezi, and S. H. Simon, Phys. Rev. X **4**, 031039 (2014).

[12] F. Grusdt, F. Letscher, M. Hafezi, and M. Fleischhauer, Phys. Rev. Lett. **113**, 155301 (2014).

[13] M. Hafezi, E. A. Demler, M. D. Lukin, and J. M. Taylor, Nat. Phys. **7**, 907 (2011).

[14] N. Y. Yao, C. R. Laumann, A. V. Gorshkov, H. Weimer, L. Jiang, J. I. Cirac, P. Zoller, and M. D. Lukin, Nat. Commun. **4**, 1585 (2013).

[15] S. Lloyd, Science **321**, 1463 (2008).

[16] R. J. Schoelkopf and S. M. Girvin, Nature(London) **451**, 664 (2008).

[17] A. A. Houck, H. E. Türeci, and J. Koch, Nature Phys. **8**, 292 (2012).

[18] M. H. Devoret and R. J. Schoelkopf, Science **339**, 1169 (2013).

[19] J. Koch, A. A. Houck, K. L. Hur, and S. M. Girvin, Phys. Rev. A **82**, 043811 (2010).

[20] A. Nunnenkamp, J. Koch, and S. M. Girvin, New J. Phys. **13**, 095008 (2011).

[21] E. Kapit, Phys. Rev. A **87**, 062336 (2013).

[22] K. M. Birnbaum, A. Boca, R. Miller, A. D. Boozer, T. E. Northup, and H. J. Kimble, Nature (London) **436**, 87 (2005).

[23] I. Fushman, D. Englund, A. Faraon, N. Stoltz, P. Petroff, and J. Vuckovic, Science **320**, 769 (2008).

[24] A. Reiserer, N. Kalb, G. Rempe, and S. Ritter, Nature (London) **508**, 237 (2014).

[25] I. Friedler, D. Petrosyan, M. Fleischhauer, and G. Kurizki, Phys. Rev. A **72**, 043803 (2005).

[26] A. V. Gorshkov, J. Otterbach, M. Fleischhauer, T. Pohl, and M. D. Lukin, Phys. Rev. Lett. **107**, 133602 (2011).

[27] Y. O. Dudin and A. Kuzmich, Science **336**, 887 (2012).

[28] V. Parigi, E. Bimbard, J. Stanojevic, A. J. Hilliard, F. Nogrette, R. Tualle-Brouri, A. Ourjoumtsev, and P. Grangier, Phys. Rev. Lett. **109**, 233602 (2012).

[29] O. Firstenberg, T. Peyronel, Q.-Y. Liang, A. V. Gorshkov, M. D. Lukin, and V. Vuletic, Nature (London) **502**, 71 (2013).

[30] D. Maxwell, D. J. Szwer, D. Paredes-Barato, H. Busche, J. D. Pritchard, A. Gauguet, K. J. Weatherill, M. P. A. Jones, and C. S. Adams, Phys. Rev. Lett. **110**, 103001 (2013).

[31] G. Günter, H. Schempp, M. Robert-de Saint-Vincent, V. Gavryusev, S. Helmrich, C. S. Hofmann, S. Whitlock, and M. Weidemüller, Science **342**, 954 (2013).

[32] S. Baur, D. Tiarks, G. Rempe, and S. Dürr, Phys. Rev. Lett. **112**, 073901 (2014).

[33] H. Gorniaczyk, C. Tresp, J. Schmidt, H. Fedder, and S. Hofferberth, Phys. Rev. Lett. **113**, 053601 (2014).

[34] N. Y. Yao, C. R. Laumann, A. V. Gorshkov, S. D. Bennett, E. Demler, P. Zoller, and M. D. Lukin, Phys. Rev. Lett. **109**, 266804 (2012).

[35] M. Kiffner, W. Li, and D. Jaksch, Phys. Rev. Lett. **110**, 170402 (2013).

[36] J. Cho, D. G. Angelakis, and S. Bose, Phys. Rev. Lett. **101**, 246809 (2008).

[37] A. E. B. Nielsen and K. Mølmer, Phys. Rev. A **82**, 052326 (2010).

[38] F. Grusdt and M. Fleischhauer, Phys. Rev. A **87**, 043628 (2013).

[39] R. O. Umucalilar and I. Carusotto, Phys. Rev. Lett. **108**, 206809 (2012).

[40] A. L. C. Hayward, A. M. Martin, and A. D. Greentree, Phys. Rev. Lett. **108**, 223602 (2012).

[41] M. Fleischhauer, A. Imamoglu, and J. P. Marangos, Rev. Mod. Phys. **77**, 633 (2005).

[42] C. Guerlin, E. Brion, T. Esslinger, and K. Mølmer, Phys. Rev. A **82**, 053832 (2010).

[43] E. Brion, F. Carlier, V. M. Akulin, and K. Mølmer, Phys. Rev. A **85**, 042324 (2012).

[44] X.-F. Zhang, Q. Sun, Y.-C. Wen, W.-M. Liu, S. Eggert, and A.-C. Ji, Phys. Rev. Lett. **110**, 090402 (2013).

[45] A. Grankin, E. Brion, E. Bimbard, R. Boddeda, I. Usmani, A. Ourjoumtsev, and P. Grangier, New J. Phys. **16**, 043020 (2014).

[46] V. Kalmeyer and R. B. Laughlin, Phys. Rev. Lett. **59**, 2095 (1987).

[47] V. Kalmeyer and R. B. Laughlin, Phys. Rev. B **39**, 11879 (1989).

[48] I. Carusotto and C. Ciuti, Rev. Mod. Phys. **85**, 299 (2013).

[49] M. Fleischhauer, S. F. Yelin, and M. D. Lukin, Opt. Commun. **179**, 395 (2000).

[50] A. V. Gorshkov, A. André, M. D. Lukin, and A. S. Sørensen, Phys. Rev. A **76**, 033804 (2007).

[51] H. Weimer, N. Y. Yao, and M. D. Lukin, Phys. Rev. Lett. **110**, 067601 (2013).

[52] Y.-F. Wang, Z.-C. Gu, C.-D. Gong, and D. N. Sheng, Phys. Rev. Lett. **107**, 146803 (2011).

[53] B. A. Bernevig and N. Regnault, Phys. Rev. B **85**, 075128 (2012).

[54] P. Schauß, M. Cheneau, M. Endres, T. Fukuhara, S. Hild, A. Omran, T. Pohl, C. Gross, S. Kuhr, and I. Bloch, Nature (London) **491**, 87 (2012).

[55] S. Zhang, F. Robicheaux, and M. Saffman, Phys. Rev. A **84**, 043408 (2011).

[56] M. J. Piotrowicz, M. Lichtman, K. Maller, G. Li, S. Zhang, L. Isenhower, and M. Saffman, Phys. Rev. A **88**, 013420 (2013).

[57] F. Nogrette, H. Labuhn, S. Ravets, D. Barredo, L. Béguin, A. Vernier, T. Lahaye, and A. Browaeys, Phys. Rev. X **4**, 021034 (2014).

[58] R. Dumke, M. Volk, T. Müther, F. B. J. Buchkremer, G. Birkl, and W. Ertmer, Phys. Rev. Lett. **89**, 097903 (2002).

[59] G. V. Vdovin, O. Akhzar-Mehr, P. M. Sarro, D. W. De Lima Monteiro, and M. Y. Loktev, Proc. SPIE **4945**, 107 (2003).

[60] M. Notcutt, L.-S. Ma, J. Ye, and J. L. Hall, Opt. Lett. **30**, 1815 (2005).

[61] A. V. Gorshkov, R. Nath, and T. Pohl, Phys. Rev. Lett. **110**, 153601 (2013).

[62] To alleviate the antiblockade effect [81,82] and the closely related singular polariton-polariton interaction potential [83], the initial preparation of one Rydberg excitation per site can be done in the presence of a red-detuned control field (i.e., $\Delta_\alpha > 0$) and repulsive van der Waals Rydberg-Rydberg interactions. In that case, the interactions cannot compensate for the $\Omega_\alpha^2/\Delta_\alpha$ Stark shift, thus avoiding the resonance.

[63] T. Pohl, E. Demler, and M. D. Lukin, Phys. Rev. Lett. **104**, 043002 (2010).

[64] P. Schauß, J. Zeiher, T. Fukuhara, S. Hild, M. Cheneau, T. Macrì, T. Pohl, I. Bloch, and C. Gross, arXiv:1404.0980.

[65] M. Barkeshli, N. Y. Yao, and C. R. Laumann, arXiv:1407.7034.

[66] J. A. Kjäll and J. E. Moore, Phys. Rev. B **85**, 235137 (2012).

[67] N. Goldman, J. Beugnon, and F. Gerbier, Phys. Rev. Lett. **108**, 255303 (2012).

[68] M. Fleischhauer and M. D. Lukin, Phys. Rev. Lett. **84**, 5094 (2000).

[69] N. Yao, C. R. Laumann, B. L. Lev, and A. V. Gorshkov (unpublished).

[70] D. Peter, N. Y. Yao, N. Lang, S. D. Huber, M. D. Lukin, and H. P. Büchler, arXiv:1410.5667 [cond-mat.quant-gas].

[71] S. Yang, Z.-C. Gu, K. Sun, and S. Das Sarma, Phys. Rev. B **86**, 241112 (2012).

[72] Z. Liu, E. J. Bergholtz, H. Fan, and A. M. Läuchli, Phys. Rev. Lett. **109**, 186805 (2012).

[73] T. Karzig, C.-E. Bardyn, N. Lindner, and G. Refael, arXiv:1406.4156 [cond-mat.quant-gas].

[74] A. V. Nalitov, D. D. Solnyshkov, and G. Malpuech, arXiv:1409.6564 [cond-mat.mes-hall].

[75] C.-E. Bardyn, T. Karzig, G. Refael, and T. C. H. Liew, arXiv:1409.8282 [cond-mat.quant-gas].

[76] B. Swingle and J. McGreevy, arXiv:1407.8203.

[77] A. V. Gorshkov, K. R. A. Hazzard, and A. M. Rey, Mol. Phys. **111**, 1908 (2013).

[78] M. Saffman, T. G. Walker, and K. Mølmer, Rev. Mod. Phys. **82**, 2313 (2010).

[79] A. V. Gorshkov, S. R. Manmana, G. Chen, J. Ye, E. Demler, M. D. Lukin, and A. M. Rey, Phys. Rev. Lett. **107**, 115301 (2011).

[80] A. V. Gorshkov, S. R. Manmana, G. Chen, E. Demler, M. D. Lukin, and A. M. Rey, Phys. Rev. A **84**, 033619 (2011).

[81] C. Ates, T. Pohl, T. Pattard, and J. M. Rost, Phys. Rev. Lett. **98**, 023002 (2007).

[82] T. Amthor, C. Giese, C. S. Hofmann, and M. Weidemüller, Phys. Rev. Lett. **104**, 013001 (2010).

[83] M. F. Maghrebi, M. J. Gullans, P. Bienias, S. Choi, I. Martin, O. Firstenberg, M. D. Lukin, H. P. Büchler, and A. V. Gorshkov (unpublished).